Atmos. Chem. Phys. Discuss., 10, 8595–8621, 2010
www.atmos-chem-phys-discuss.net/10/8595/2010/

Atmospheric Chemistry and Physics Discussions

This discussion paper is/has been under review for the journal Atmospheric Chemistry and Physics (ACP). Please refer to the corresponding final paper in ACP if available.

Particle size distributions from laboratory-scale biomass fires using fast response instruments

S. Hosseini[1], L. Qi[1], D. Cocker[1], D. Weise[2], A. Miller[3], M. Shrivastava[1,4], W. Miller[1], S. Mahalingam[1], M. Princevac[1], and H. Jung[1]

[1]University of California, Riverside, CA 92521, USA
[2]USDA Forest Service, Pacific Southwest Research Station, Forest Fire Laboratory, Riverside, CA, USA
[3]National Institutes for Occupational Safety and Health (NIOSH), GA, USA
[4]Pacific Northwest National Laboratory, Richland, WA, USA

Received: 28 February 2010 – Accepted: 8 March 2010 – Published: 6 April 2010

Correspondence to: H. Jung (heejung@engr.ucr.edu)

Published by Copernicus Publications on behalf of the European Geosciences Union.

Abstract

Particle size distribution from biomass combustion is an important parameter as it affects air quality, climate modelling and health effects. To date particle size distributions reported from prior studies vary not only due to difference in fuels but also difference in experimental conditions. This study aims to report characteristics of particle size distribution in a well controlled repeatable lab scale biomass fires for southwestern US fuels. The combustion facility at the USDA Forest Service's Fire Science Laboratory (FSL), Missoula, MT provided repeatable combustion and dilution environment ideal for particle size distribution study. For a variety of fuels tested the major mode of particle size distribution was in the range of 29 to 52 nm, which was attributable to dilution of the fresh smoke. Comparing volume size distribution from Fast Mobility Particle Sizer (FMPS) and Aerodynamic Particle Sizer (APS) measurements, ~30% of particle volume was attributable to the particles ranging from 0.5 to 10 µm for PM_{10}. Geometric mean diameter rapidly increased during flaming and gradually decreased during mixed and smoldering phase combustion. Most of fuels gave unimodal distribution during flaming phase and strong biomodal distribution during smoldering phase. The mode of combustion (flaming, mixed and smoldering) could be better distinguished using slopes in Modified Combustion Efficiency (MCE) vs. geometric mean diameter from each mode of combustion than only using MCE values.

1 Introduction

Biomass combustion encompasses a wide range of sources including wildland fire, prescribed burning, agricultural residue/waste burning, residential wood combustion, and power generation. Since the 1970s, considerable effort has been devoted to characterizing the products associated with biomass combustion in general. In the United States, intentional biomass burning (prescribed burning) is regulated by the Clean Air Act. Prescribed burning is the planned use of fire under specified environmental and

ACPD

10, 8595–8621, 2010

meteorological conditions to accomplish specific vegetation management objectives. These objectives include the removal of hazardous fuel accumulations, wildlife habitat improvement, forest regeneration, and mimicking the natural role of fire. In order to utilize prescribed burning, managers must provide estimates of the quantity of certain combustion products that will be produced before air quality regulators issue burn permits. These products of combustion include particulate matter (PM) released into the atmosphere (Chi, 1979; Levine, 1996; Goldammer, 2009). Particles can affect the radiation budget of the earth depending on their size distribution, morphology and chemical composition. There is growing evidence of the role of particle size distribution and its adverse effect on human health following transport and deposition of particles (Pope and Dockery, 2006). Currently in the US, the production of particles with mean diameter equal or below 2.5 µm is regulated due to the adverse impacts on human health and visibility.

Particle size distribution from biomass combustion evolves due to condensation/coagulation within the plume and photochemical aging downstream of the fire. The particle size distribution can also differ by combustion phase (ignition/flaming/smoldering), fuel condition (live, dead and varying moisture content), fuel configuration (dense vs. light and plain vs. sloped terrain), and fuel types (foliage, log, branch). Due to the importance of particle size distribution and its impact on air quality, climate modeling and health effects, particle size distributions from diverse biomass combustion conditions have been reported (Janhall, 2009; Hays et al., 2005; Capes et al., 2008).

Particle size distributions from biomass burning have been studied for a variety of fuels (Le Canut, 1996; Posfai et al., 2003, 2004; Capes et al., 2008), A wide variety of instruments have been used to measure particle size distribution,: laser optical particle counter, Aerosol Time-Of-Flight Mass Spectrometer (ATOFMS), Differential Mobility Particle Sizer (DMPS) (Hedberg et al., 2002; Sullivan et al., 2008), Scanning Mobility Particle Sizer (Hays et al., 2002, 2005), Transmission Electron Microscopy (TEM) analysis (Posfai et al., 2003, 2004; Chakrabarty et al., 2006), Micro Orifice Uniform Deposit

ACPD
10, 8595–8621, 2010

Impactor (MOUDI) (Hays et al., 2005; Engling et al., 2009), and Passive Cavity Aerosol Spectrometer Probe (PCASP) (Capes et al., 2008).

Previous studies have shown a wide variation in particle size distribution due to different combustion and measurement conditions. Hays et al. (2002) reported unimodal distribution using a SMPS. They had an open combustion of a fuel to simulate combustion of fuel in the field. They reported geometric mean diameter between 0.1–0.2 µm. Due to the use of a small enclosure (28 m^3), their particles must have grown by condensation and coagulation within the enclosure. Le Canut et al. (1996) measured particle size distribution using a laser optical counter in their airborne study during a savanna fire. They reported two mass modes: one in 0.2–0.3 µm and the other above 2 µm. Chakrabarty et al. (2006) measured particle size distribution from laboratory combustion of eight different fuels using SMPS and image analysis. Projected area equivalent diameter peaks ranged from 30 to 200 nm. To authors' knowledge none of previous studies captured the temporal evolution of size distribution due to the relatively slow response rate of the instruments. For example, the SMPS requires 2 min to measure one size distribution. Janhäll et al. (2009) parameterized particle number emissions by applying complicated fittings to published experimental data. They pointed out that well defined laboratory experiments should help validate their finding and enable a better understanding of particle emission/formation mechanisms.

A study to characterize smoke emissions from prescribed burns in chaparral and Madrean oak woodlands in the southwestern United States was initiated in 2008. Detailed characterization of gaseous and particulate emissions is being made in laboratory and field settings. Changes in transport of emissions from the source downwind are being measured and modeled for inclusion in air quality models such as CMAQ (Byun, 2006). The objective of this paper is to characterize particle size distribution from the laboratory component of the study. A suite of fast-response online instruments were applied to measure evolution of particle size distribution from fire ignition to extinction to capture transient and integrated characteristics of particle size distribution from biomass burning. To the best of our knowledge, current study reports fast

ACPD
10, 8595–8621, 2010

time-dependent (1s interval) size distribution of the particle-phase emissions and their characteristics from biomass burning in detail for the first time.

2 Experimental

2.1 Combustion lab facility

Experiments were conducted in the combustion laboratory at the USDA Forest Service's Fire Science Laboratory (FSL), Missoula, MT. A detailed description of the characteristics of the facility can be found in Christian et al. (2004). The facility measures 12.5 m by 12.5 m and is 22 m in height. The combustion laboratory is exhausted via a 3.6 m diameter hood attached to a 1.6 m stack located in the center. Figure 1 shows a schematic of the lab. The base of the hood is above the fuel bed. The stack extends from 2 m above the floor to all the way up through the ceiling. The lab is slightly pressurized with pre-conditioned outside air to precisely control the temperature, and relative humidity. This ensures entrainment of all the produced emissions, making the conditions ideal for determining emission factors. The air velocity in the chimney was set at either 1.5 m/s or 3 m/s by controlling the exhaust fan speed to maintain proper entrainment of fresh air.

2.2 Particle measurement system

The sampling platform (Fig. 1) is located 17 m above the floor surrounding the stack; this is where all particle measurement instruments were placed. Figure 2 shows schematics of sampling system. First sampling flow was taken from the isokinetic sampling port installed at the height of the sampling platform at the stack. The sample flow was diluted using a mini dilution tunnel at 13.5:1 ratio. The diluted aerosol flow directed to a PM_{10} impactor, then distributed to Fast Mobility Particle Sizer (FMPS-model 3091,

ACPD
10, 8595–8621, 2010

TSI[1]), an Aerodynamic Particle Sizer (APS-model 3321, TSI) and Condensation Particle Counter (CPC Model 3776, TSI). Other online and offline instruments were used for physical and chemical characterization of the particles but are not reported in this paper.

2.3 Gas measurement system

An Open-Path Fourier Transform infrared (OP-FTIR) spectrometer was used to monitor concentrations of CO and CO_2. These concentrations were used to calculate a Modified Combustion Efficiency (MCE). MCE is defined as the amount of carbon released as CO_2 divided by the amount of carbon released as CO_2 plus CO (Ward et al., 1996; Ward, 1993):

$$\mathrm{MCE} = \frac{\Delta CO_2}{\Delta CO_2 + \Delta CO}$$

$$\Delta x = x_{\mathrm{measured}} - x_{\mathrm{background}} \quad (1)$$

Since CO_2 and CO account for about 95% of carbon released during biomass combustion, the MCE is an excellent surrogate for true combustion efficieny. Ward (1993) classified combustion conditions by MCE: flaming phase when MCE>0.97, mixed phase when 0.85<MCE<0.97 and smoldering phase when 0.75<MCE<0.85.

2.4 Experimental combustions

Fuel characterization and fuel bed configuration are very important parameters to determine particle emissions and formations. Yet many previous studies are lacking this critical information in their publications (Reid et al., 2005). In the present work, a total of 49 burns, composed of 9 different types of wildland fuels (Table 1), were conducted. The fuels were collected from California (Ft. Hunter-Liggett, Vandenberg Air

[1]The use of trade names is provided for informational purposes only and does not constitute endorsement by the US Department of Agriculture.

ACPD
10, 8595–8621, 2010

Force Base) and Arizona (Ft. Huachuca). The fuel types selected for study are primarily living fuels when burned in the field. Chaparral is a name used to describe mixtures of shrub species that grow together in California. Chaparral grows in areas of relatively shallow soil and limited moisture (Keeley, 1999; Christensen, 1999). Even though the areas where these shrubs grow are quite different, these shrub assemblages have developed similar physical characteristics such as leaves with waxy cuticles which pyrolyze at low temperatures (Susott, 1982) and canopy structure that facilitates fire spread in the crowns. Fires burning in these fuel beds are typically intense with relatively high rates of energy release. The oak woodland type consists of oak trees with an understory of shrub species.

Small amount of isopropyl alcohol was used initially to get a quick even ignition of the fuel bed. Eighteen of 49 of the southwestern fuel beds (chamise, ceanothus, manzanita, and California sagebrush) were ignited in this manner using a propane torch. No alcohol was used to enhance ignition in the remaining fuel beds. With the exception of masticated mesquite fuel type, the fuels tend to have a vertical orientation in the natural setting as in Fig. 3a. We attempted to burn the fuels in this orientation with limited success so the fuels were oriented horizontally (Fig. 3b). Bulk characteristics of the fuel beds are found in Table 2. Average moisture content (oven-dry mass basis, ASTM D4442-07) of the fuel beds at the time of burning ranged from 4 to 33% which is similar to fuel moistures in dead fuels. Note that in the case of live fuels moisture content seldom drops below 50%. The initial oven-dry mass in the fuel beds ranged from about 670 to 4630 g. Bulk density of the fuel beds ranged from 5.8 to 14 kg/m^3 and the packing ratio (defined as the ratio of fuel bulk density to fuel density) ranged from 0.010 to 0.024. These packing ratios for the southwestern fuels are similar to those reported for laboratory fire spread experiments (Weise et al., 2005), but they are 1 to 2 orders of magnitude larger than packing ratios observed in the field. The arrangement of the fuels for burning significantly affected fuel consumption. We attempted to arrange the chamise/scrub oak fuels vertically as found in nature (Fig. 3a), but the fuels did not burn well because the fire failed to spread resulting in average consumption of

ACPD
10, 8595–8621, 2010

30% (mass basis) for this fuel type. The fuel beds for the remaining fuel types were arranged horizontally (Fig. 3b) which greatly increased fuel consumption to 90% for all other fuel types except for ceanothus. Three of the ceanothus fuel beds were burned vertically with consumption ranging from 3 to 52% and three were burned horizontally with consumption ranging from 77 to 93%.

3 Results and discussion

3.1 Particle size distribution from 7 to 520 nm measured by FMPS

Figure 4a shows averaged particle size distribution for different fuels measured by FMPS. The size distribution is averaged over the time from ignition to the end of sampling (absolute CO concentration 1 ppm) and over three repeated burning for each fuel. Averaged size distributions were unimodal for many fuel types. Interestingly, a few fuel types show distinguishable biomodal distribution, with the minor (meaning lower concentration) mode around 10 nm. The major mode varies from 29 to 52 nm for fuels tested. This is a very narrow range considering diverse fuels tested. The similarity of the size distribution among fuels tested can be attributable to the systematic burning and sampling method. The fuel was arranged to ensure that the burning is similar to actual or real burning condition in the prescribed burn. The combustion facility in Missoula was designed to divert all the generated smoke into the chimney. This allows enough dilution of the particles so that particle sizes measured and reported in this facility are smaller than those from other studies. Chakrabarty et al. (2006) used the same combustion facility in Missoula for their experiment. They reported particle Count Median Diameter (CMD) varying from 30 to 70 nm for dry fuels (sage brush, poplar wood, ponderosa pine wood, ponderosa pine needles, white pine needles, Montana grass, dambo grass, tundra core) but they found the CMD increased to 120–140 nm for wet fuels (tundra core and Montana grass) from their SEM measurement. Hays et al. (2005) measured size distribution from open burning of agricultural biomass (wheat

ACPD
10, 8595–8621, 2010

straw). The open burning was conducted in an enclosure and the particles were diluted from 1:25 to 36 and measured by a SMPS. They reported a biomodal distribution and suggested that one mode is characterized by nucleation while the other represents an accumulation mode. The modes in their size distributions were around 100 nm. Their SMPS scan measurement takes 60 to 120 s. Considering characteristics of biomass burning this is not fast enough to capture the transient phenomena. The background particle size distribution was obtained by averaging size distribution measured before ignitions for seven burns which were conducted consecutively in one experimental day and plotted with averaged size distributions in log scale as shown in Fig. 4b. Figure 4b also shows particle concentration decreases sharply above 200 nm.

While some other studies report combustion conditions of biomass burn only by using integrated or averaged MCE over the whole burn, we attempted to segregate the mode of combustion during each burn using instantaneous MCE value and other indicator. The average size distributions of Fig. 4a, b were segregated into three burning conditions: flaming, mixed and smoldering by MCE. This division was done by plotting geometric diameter change as a function of MCE instead of using only Ward and Radke's criteria by MCE value. Details of this will be discussed in later section. The majority of particles were emitted during flaming therefore the shapes of size distribution during flaming were similar to that of the average of the whole burn (Fig. 4c). (Note our presentation of data in Fig. 4 is time based while some studies report particle emission per fuel mass.) Mixed burn, which is post flaming and pre smoldering, shows unimodal distribution with the mode ranges from 30 to 50 nm (Fig. 4d). The particle concentration was lower than that of flaming by factor of 5 roughly. The change between flaming and mixed mode could be observed clearly from our video recording of all burns. The size of flames was decreased noticeably at the beginning of the mixed burn compared to that of the flaming burn. The flame was still clearly visible during the mixed burn.

Size distribution from smoldering showed bimodal distribution for all fuel types around 10 nm (Fig. 4e). It is possible that there is nucleation of volatile particles as

ACPD
10, 8595–8621, 2010

the burnt gas temperature cooled down. The particle concentration is two orders of magnitude lower than that of flaming. Note that this is time based not per fuel mass based. Analysis per fuel mass based will be reported as a separate paper. Figure 4f shows background particle size distribution change during a day. The background concentrations (Fig. 4f) are much lower than our measured particle concentration during the burn (Fig. 4c, d, e), which ensures that background particles did not interfere our measurements. Table 3 shows geometric diameter and standard deviation of size distributions for fuels tested.

3.2 Particle size distribution from 500 nm to 20 µm measured by APS

Figure 5a shows time and cycle averaged particle size distributions from APS measurement. This is to determine whether large particle concentrations are higher than background aerosol by number and by volume. It has been reported that mass mean diameter is as large as 0.5 µm for aged particles from biomass burning (Reid et al., 2005). Most of these previous measurements were performed optically on aircraft. Particles larger than 100 nm in mobility diameter were reported by previous studies which measured size distribution in the field. However smaller particle mode was reported for particles measured in the lab (Hays et al., 2005; Keshtkar and Ashbaugh, 2007). This can be attributed to immediate dilution which prevents further coagulation and condensation. Regardless, particles larger than 500 nm were measured using APS to determine whether there is any noticeable number or mass of particles in this size range from freshly diluted biomass smoke. Particle number distribution in Fig. 5a shows that the concentrations are orders of magnitude lower compared to small particles measured by FMPS. Figure 5b is the logscale graph of Fig. 5a. This shows measured distributions are greater than that of background. Background distributions (Fig. 5f) measured between each burn during a day show that they do not vary much compared to that of small size particles (Fig. 4f). This validates that our APS measurement were not interfered by background particle size distribution. The average size distributions of Fig. 5a, b were separated into three conditions: flaming (Fig. 5c), mixed

ACPD
10, 8595–8621, 2010

(Fig. 5d) and smoldering (Fig. 5e) by using the same method as FMPS size distribution. Particles larger than 500 nm were emitted mostly during flaming and mixed phases of combustion. Emissions during smoldering phase are lower by at least a factor of 4 in-comparison to peak concentrations. The volume distributions were compared between large and small particles measured by APS and FMPS. Figure 6 shows that the particles larger than 0.5 µm attribute to ~30% of total volume measured by APS and FMPS. Note the size distribution by APS is in aerodynamic diameter while that by FMPS is in mobility diameter. Note that particle health effects are assessed by $PM_{2.5}$ (particles smaller than 2.5 µm). Filter samples were taken for $PM_{2.5}$ and reported elsewhere in conjunction with the current study.

3.3 Evolution of particle size distribution (FMPS+APS)

It is extremely difficult to identify rules which determine evolution of particle distribution from biomass burning due to the large variance in fuel composition, fuel humidity, fuel bed arrangement and the nature of turbulent combustion. Therefore most of previous studies reported either time integrated results or snap shots of transient phenomenon. In order to gain an understanding of the evolution of particle size distribution, it is instructive to examine Fig. 7 which shows the evolution of particle size distribution for a burn from initial ignition until extinction. This temporal resolution is possible due to the fast scanning ability of the FMPS and the APS (1 scan per second). The data shows that particle concentration reaches a maximum during the flaming phase (confirmed by CO and CO_2 data) and diminishes to lower concentration either in unimodal, or bimodal distributions. Peak concentration measured by FMPS showed at least four orders of magnitude higher value than that of APS during flaming and mixed phase. Likewise, the evolution of number geometric mean diameter was plotted for a few burns as illustrated in Fig. 8. These results reveal that the geometric mean diameter increases rapidly during flaming phase and decreases during mixed and smoldering phases. In Fig. 9, MCE is plotted as a function of geometric diameter for three different fuels. By comparing video records of the burn with Fig. 9, we find that the change in combustion

mode is related to the change in slope in the geometric mean diameter vs. MCE curve. The geometric mean diameter increases rapidly during flaming condition when MCE is ~1. However, MCE value for mixed phase could become smaller than what Ward and Radke (1993) defined. The geometric mean diameter decreases during both mixed and smoldering conditions. While the MCE decreases as the mixed phase proceeds, the MCE value increases as the smoldering phase proceeds. As a result one can distinguish mixed phase combustion from smoldering phase combustion. We found this is better index than following Ward and Radke's criteria by MCE value.

4 Conclusions

This paper characterizes particle size distribution from the laboratory scale biomass fires for a variety of southwestern US fuels including chaparral. A suite of fast-response online instruments were applied to measure evolution of particle size distribution from fire ignition to extinction to capture transient and integrated characteristics of particle size distribution from biomass burning. Time averaged particle size distributions were segregated into three combustion modes: flaming, mixed and smoldering mode. The major mode of particle size distribution was in the range of 29 to 52 nm for the cycle averaged distribution. This is much smaller size compared to previous studies in the field study. The difference from previous studies can be attributable to dilution of the fresh smoke in the current study. Time averaged partcle concentrations were highest during flaming phase and they gradually decreased during mixed and smoldering phase. Comparing volume size distribution from FMPS and APS measurement, ~30% of particle volume was attributable to the particles ranging from 0.5 to 10 μm for PM_{10}. Geometric mean diameter rapidly increased during flaming and gradually decreased during mixed and smoldering phase combustion. Most of fuels gave unimodal distribution during flaming phase and strong biomodal distribution during smoldering phase. The mode of combustion (flaming, mixed and smoldering) could be better distinguished using slopes in MCE vs. geometric mean diameter from each mode of combustion

ACPD
10, 8595–8621, 2010

than only using MCE values. To the best of our knowledge, current study reports fast time-dependent (1s interval) size distribution of the particle-phase emissions and their characteristics from biomass burning in detail for the first time.

Acknowledgements. Funding for this study was provided by the US Department of Defence Strategic Environmental Research and Development Program as projects SI-1647, SI-1648, and SI-1649. We appreciate the assistance of personnel at USMC Camp LeJuene, US Army Ft. Huachuca, Ft. Hunter-Liggett, Ft. Benning, and Vandenberg Air Force Base in selecting fuel types for study and fuel samples for burning. Authors are grateful to Robert Yokelson and Ian Burling for FTIR data and WeiMin Hao, Shawn Urbanski, Cyle Wold, Joey Chong, Trevor Maynard and Emily Lincoln for their help.

References

Byun, D. W. and Schere, K. L.: Review of Governing equations, Computational Algorithms, and Other Components of the Models-3 Community Multi-scale Air Quality (CMAQ) Modeling Systems, Appl. Mech. Rev., 59, 51–77, 2006.

Capes, G., Johnson, B., McFiggans, G., Williams, P. I., Haywood, J., and Coe, H.: Aging of biomass burning aerosols over West Africa: Aircraft measurements of chemical composition, microphysical properties, and emission ratios, J. Geophys. Res.-Atmos., 113, D00c15, doi:10.1029/2008jd009845, 2008.

Chakrabarty, R. K., Moosmuller, H., Garro, M. A., Arnott, W. P., Walker, J., Susott, R. A., Babbitt, R. E., Wold, C. E., Lincoln, E. N., and Hao, W. M.: Emissions from the laboratory combustion of wildland fuels: Particle morphology and size, J. Geophys. Res.-Atmos., 111, D07204, doi:10.1029/2005jd006659, 2006.

Chi, C. T., Horn, D. A., Reznik, R. B., Zanders, D. L., Opferkuch, R. E., Nyers, J. M., Pierovich, J. M., Lavdas, L. G., Mcmahon, C. K., Nelson, R. M., Johansen, R. W., and Ryan, P. W.: Source assessment: prescribed burning, state of the art., US Environmental Protection Agency, Washington D.C., 1979.

Christensen, N. L.: Vegetation of thesoutheastern costal plain, in: North American Terrestial Vegetation, edited by: Barbour, M. G. W. D. B., Cambridge University Press, United Kingdom, 1999.

Christian, T. J., Kleiss, B., Yokelson, R. J., Holzinger, R., Crutzen, P. J., Hao, W. M., Shirai, T., and Blake, D. R.: Comprehensive laboratory measurements of biomass-burning emissions: 2. First intercomparison of open-path FTIR, PTR-MS, and GC- MS/FID/ECD, J. Geophys. Res.-Atmos., 109, D02311, doi:10.1029/2003jd003874, 2004.

Countryman, C. M.: Physical characteristics of some northern California brush fuels., USDA Forest Serivce, Pacific Southwest Forest and Range Experiment Station, General Technical Report 1982.

Engling, G., Lee, J. J., Tsai, Y. W., Lung, S. C. C., Chou, C. C. K., and Chan, C. Y.: Size-Resolved Anhydrosugar Composition in Smoke Aerosol from Controlled Field Burning of Rice Straw, Aerosol Sci. Technol., 43, 662–672, 2009.

Goldammer, J. G., Statheropoulos, M., and Andreae, M. O., Goldammer, J. G., Statheropoulos, M., and Andreae, M. O.: Impacts of vegetation fire emissions on the environment, human health, and security: a global perspective, in: Wildland Fires and Air Pollution, edited by: Bytnerowicz, A., Arbaugh, M., Riebau, A., and Andersen, C., Elsevier, 2009.

Hays, M. D., Geron, C. D., Linna, K. J., Smith, N. D., and Schauer, J. J.: Speciation of gas-phase and fine particle emissions from burning of foliar fuels, Environ. Sci. Technol., 36, 2281–2295, 2002.

Hays, M. D., Fine, P. M., Geron, C. D., Kleeman, M. J., and Gullett, B. K.: Open burning of agricultural biomass: Physical and chemical properties of particle-phase emissions, Atmos. Environ., 39, 6747–6764, 2005.

Hedberg, E., Kristensson, A., Ohlsson, M., Johansson, C., Johansson, P. A., Swietlicki, E., Vesely, V., Wideqvist, U., and Westerholm, R.: Chemical and physical characterization of emissions from birch wood combustion in a wood stove, Atmos. Environ., 36, 4823–4837, 2002.

Keeley, J. E.: Chaparral, in: North American Terrestrial Vegetation, edited by: Barbour, M. G. and Billing, W. D., Cambridge University Press, N.Y., 397–448, 1999.

Keshtkar, H. and Ashbaugh, L. L.: Size distribution of polycyclic aromatic hydrocarbon particulate emission factors from agricultural burning, Atmos. Environ., 41, 2729–2739, 2007.

Levine, J. S.: Biomass Burning and Global Change, MIT Press, 1996.

Le Canut, P., Andreae, M. O., Harris, G. W., Wienhold, F. G., and Zenker, T.: Airborne studies of emissions from savanna fires in southern Africa, J. Geophys. Res.-Atmos., 8483, doi:10.1029/2002jd002291, 1996.

Pope, C. A. and Dockery, D. W.: Health effects of fine particulate air pollution: Lines that

connect, J. Air Waste Manage., 56, 709–742, 2006.
Posfai, M., Simonics, R., Li, J., Hobbs, P. V., and Buseck, P. R.: Individual aerosol particles from biomass burning in southern Africa: 1. Compositions and size distributions of carbonaceous particles, J. Geophys. Res.-Atmos., 108, D06213, doi:10.1029/2003jd004169, 2003.
Posfai, M., Gelencser, A., Simonics, R., Arato, K., Li, J., Hobbs, P. V., and Buseck, P. R.: Atmospheric tar balls: Particles from biomass and biofuel burning, J. Geophys. Res.-Atmos., 109, D22302, doi:10.1029/2008jd010216, 2004.
Reid, J. S., Koppmann, R., Eck, T. F., and Eleuterio, D. P.: A review of biomass burning emissions part II: intensive physical properties of biomass burning particles, Atmos. Chem. Phys., 5, 799–825, 2005, http://www.atmos-chem-phys.net/5/799/2005/.
Janhäll, S., Andreae, M. O., and Pöschl, U.: Biomass burning aerosol emissions from vegetation fires: particle number and mass emission factors and size distributions, Atmos. Chem. Phys., 10, 1427–1439, 2010, http://www.atmos-chem-phys.net/10/1427/2010/.
Sullivan, A. P., Holden, A. S., Patterson, L. A., McMeeking, G. R., Kreidenweis, S. M., Malm, W. C., Hao, W. M., Wold, C. E., and Collett, J. L.: A method for smoke marker measurements and its potential application for determining the contribution of biomass burning from wildfires and prescribed fires to ambient PM2.5 organic carbon, J. Geophys. Res.-Atmos., 113, D22302, doi:10.1029/2008jd010216, 2008.
Susott, R. A.: Characterization of the thermal properties of forest fuels by combustible gas analysis., Forest Sci., 28, 404–420, 1982.
Ward, D. E., Hao, W. M., Susott, R. A., Babbitt, R. E., Shea, R. W., Kauffman, J. B., and Justice, C. O.: Effect of fuel composition on combustion efficiency and emission factors for African savanna ecosystems, J. Geophys. Res.-Atmos., 101, 23569–23576, 1996.
Ward, D. E. and Radke, L. E.: Emission measurements from vegetation fires: a comparative evaluation of methods and results, in: Fire in Environment. The Ecological, Atmospheric and Climatic Importance of Vegetation Fires, edited by: Crutzen, P. J. and Goldammer, J. G., John Wiley and Sons, New York, pp. 53–76, 1993.
Weise, D. R., Zhou, X. Y., Sun, L. L., and Mahalingam, S.: Fire spread in chaparral – 'go or no-go?', Int. J. Wildland Fire, 14, 99–106, 2005.

Table 1. Fuel type compositions and abbreviations.

Fuel type	Fuel code	Plant species
Chamise	chs	*Adenostoma fasciculatum*, *Quercus berberidifolia*
Ceanothus	cea	*Ceanothus leucodermis*
Maritime chaparral	mch	*Ceanothus impressus* var. *impressus*, *C. cuneatus* var. *fascicularis*, *Salvia mellifera*
Coastal sage scrub	cos	*Salvia mellifera*, *Ericameria ericoides*, *Artemisia californica*
California sagebrush	cas	*Artemisia californica*, *Ericameria ericoides*
Manzanita	man	*Arctostaphylos rudis*, *Arctostaphylos purissima*
Oak savanna	oas	*Quercus emoryi*, *Eragrostis lehmanniana*
Oak woodland	oaw	*Quercus emoryi*, *Arctostaphylos pungens*
Masticated mesquite	mes	*Prosopis velutina*, *Baccharis sarothroides*

Table 2. Fuel and bed properties.

Fuel type	*n*	Moisture content (%)	Fuel bed dry mass (g)	Bulk density (kg/m^3)	Packing ratio[a]	Consumption (%)
Southwestern U.S.						
Chamise/Scrub Oak	6	11.9	2079	8.6	0.015	38
Ceanothus	6	10.2	2007	5.8	0.010	54
Maritime Chaparral	5	11.2	2871	7.5	0.013	95
Coastal Sage Scrub	5	9.3	2299	6.0	0.010	95
California Sagebrush	6	9.0	2460	6.4	0.011	93
Manzanita	6	12.6	2906	7.6	0.013	94
Oak Savanna	5	14.3	2788	7.3	0.012	91
Oak Woodland	5	32.8	2054	5.3	0.009	95
Masticated Mesquite	5	4.3	1831	14.3	0.024	92

[a] Packing ratio = bulk density/particle density. Assumed particle density of 593 kg m^{-3} (average from Countryman, 1982)

ACPD
10, 8595–8621, 2010

Table 3. Geometric mean diameter and the geometric standard deviations.

Fuel type	In total	
	D_g (nm)	σ
CAS	50.72	1.66
CEA	39.67	1.64
CHS	52.30	1.62
COS	45.30	1.62
MAN	39.20	1.62
MES	34.00	1.58
OAS	25.00	1.76
OAW	29.00	1.67

ACPD
10, 8595–8621, 2010

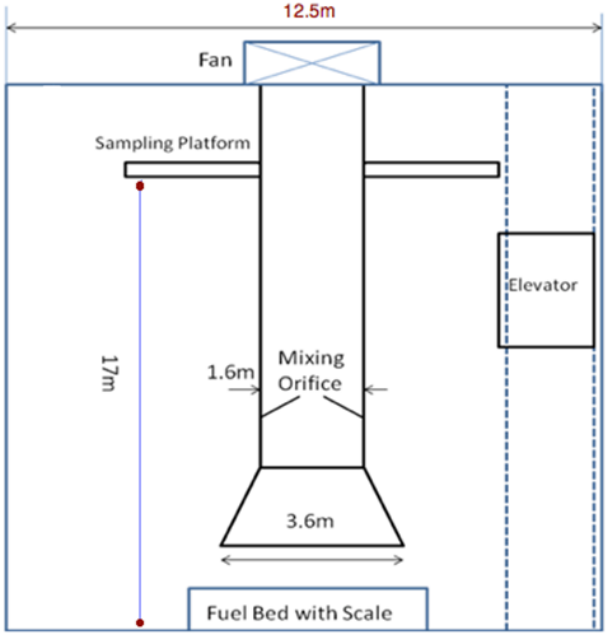

Fig. 1. Schematic drawing of combustion laboratory, USDA Forest Service Fire Sciences Laboratory, Missoula, MT. Detailed characteristics of facility are described in Christian et al. (2004).

ACPD
10, 8595–8621, 2010

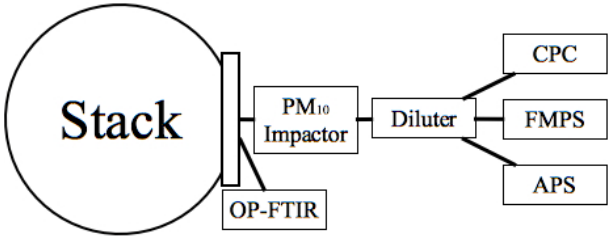

Fig. 2. Schematic of measurement system.

ACPD
10, 8595–8621, 2010

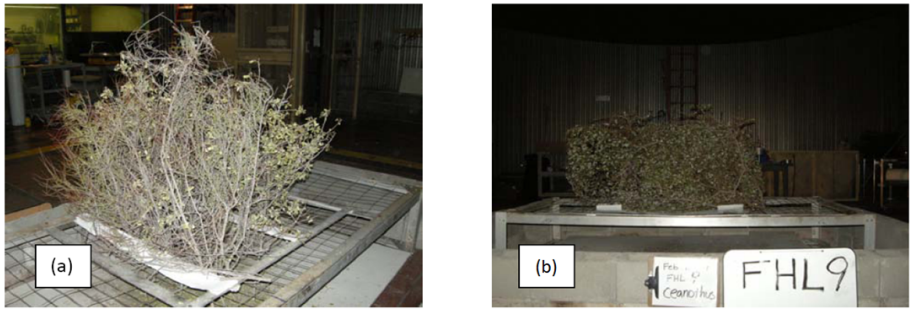

Fig. 3. Two pictures showing fuel and fuel bed, before the fuel is lit on fire.

ACPD
10, 8595–8621, 2010

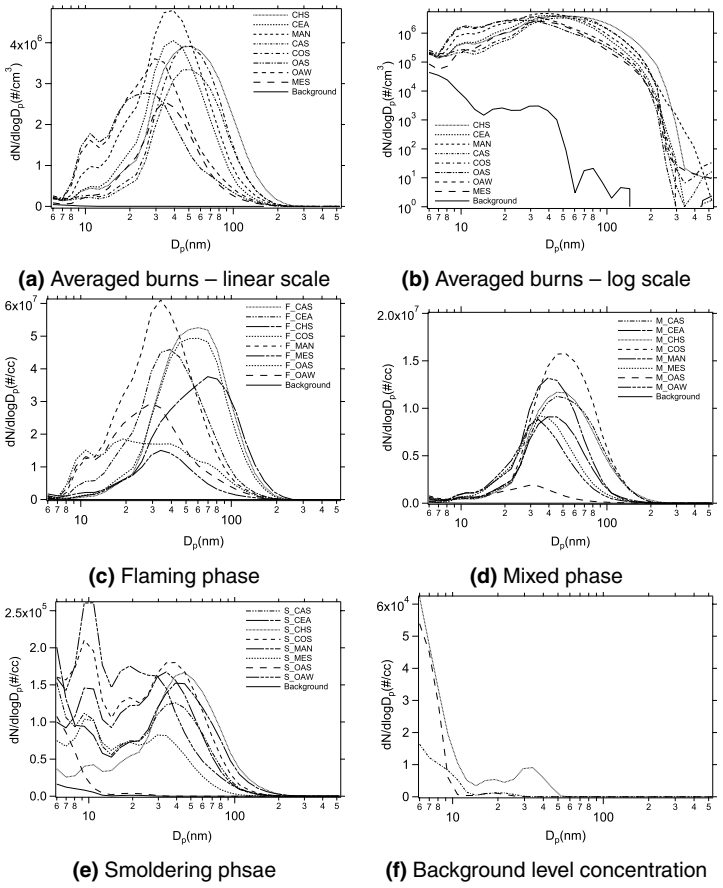

Fig. 4. Particle size distributions corresponding to **(a)** whole burn(linear), **(b)** whole burn(log-log), **(c)** flaming, **(d)** mixed, and **(e)** smoldering phases. **(f)** presents background levels measured by FMPS.

ACPD
10, 8595–8621, 2010

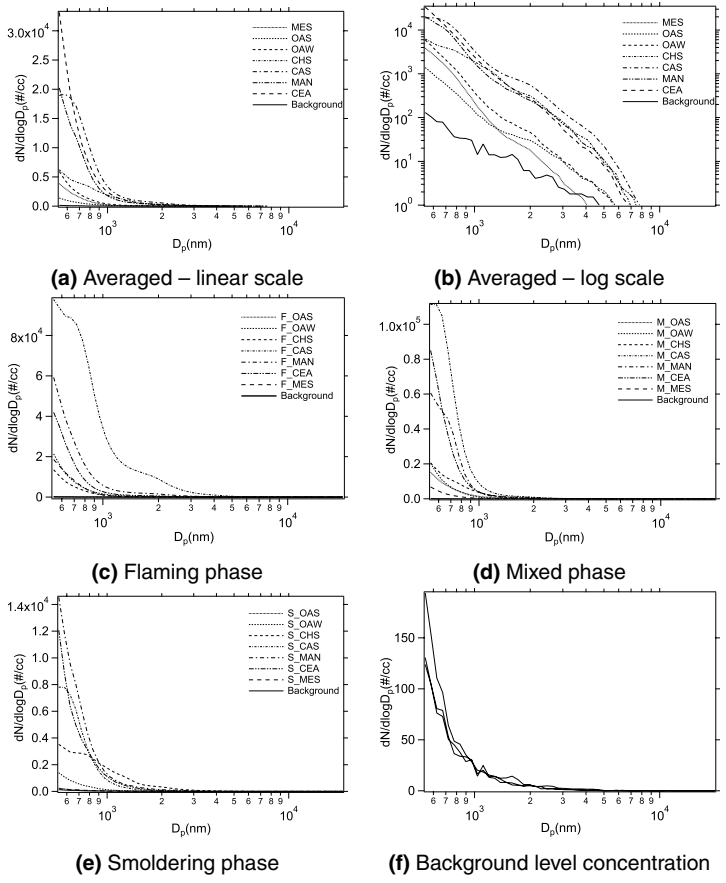

Fig. 5. Aerodynamic particle size distribution measured by APS for different phases **(a)** whole burn (linear), **(b)** whole burn (log-log), **(c)** flaming, **(d)** mixed, **(e)** smoldering, and **(f)** corresponds to background concentration.

ACPD
10, 8595–8621, 2010

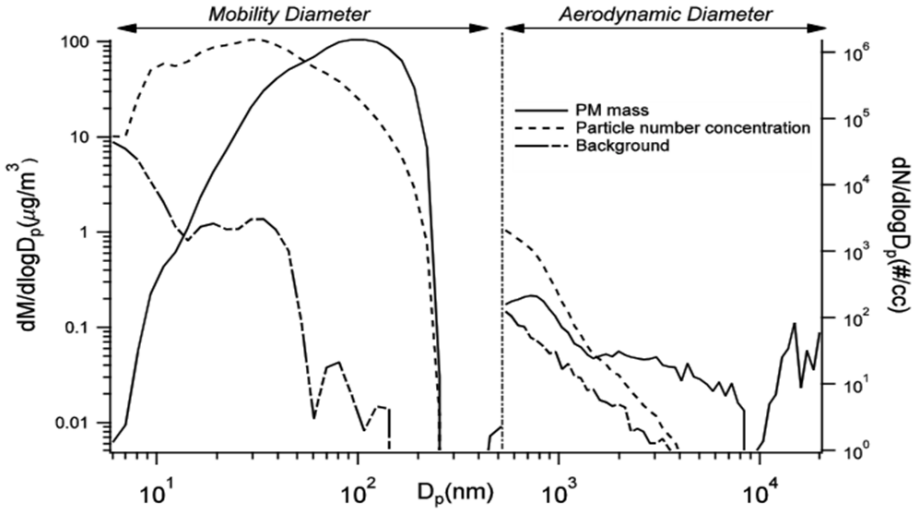

Fig. 6. Particle number and mass size distributions corresponding to a typical burn, also the background concentration.

ACPD
10, 8595–8621, 2010

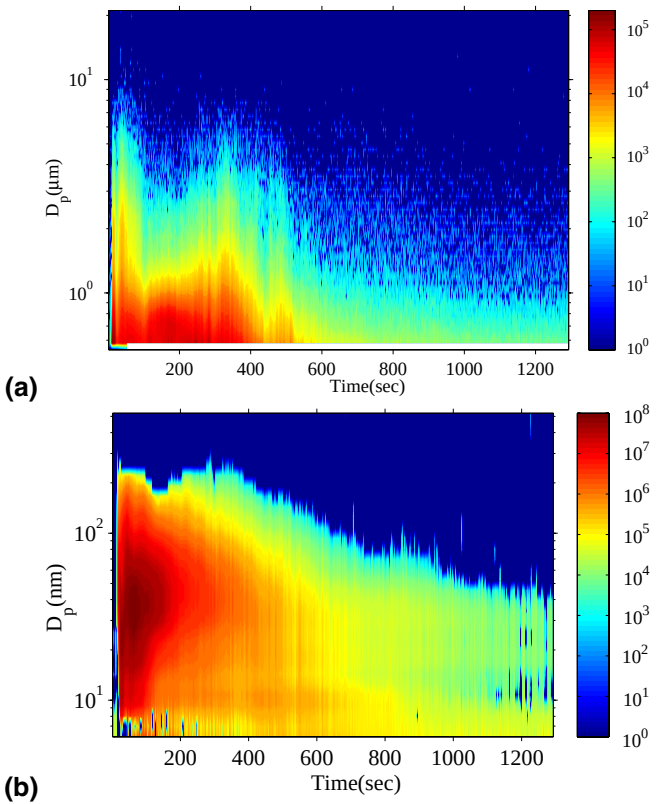

Fig. 7. APS **(a)** and FMPS **(b)** Contour graphs showing particle number size distributions.

ACPD
10, 8595–8621, 2010

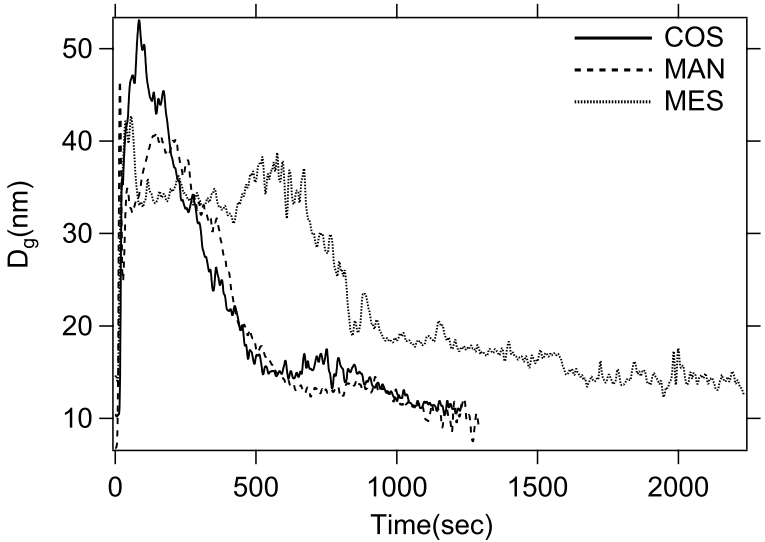

Fig. 8. Geometric Mean Diameter as a function of time for a few burns: **(a)** Manzanita (MAN), **(b)** Mesquite (MES), **(c)** Coastal Sage (COS).

ACPD
10, 8595–8621, 2010

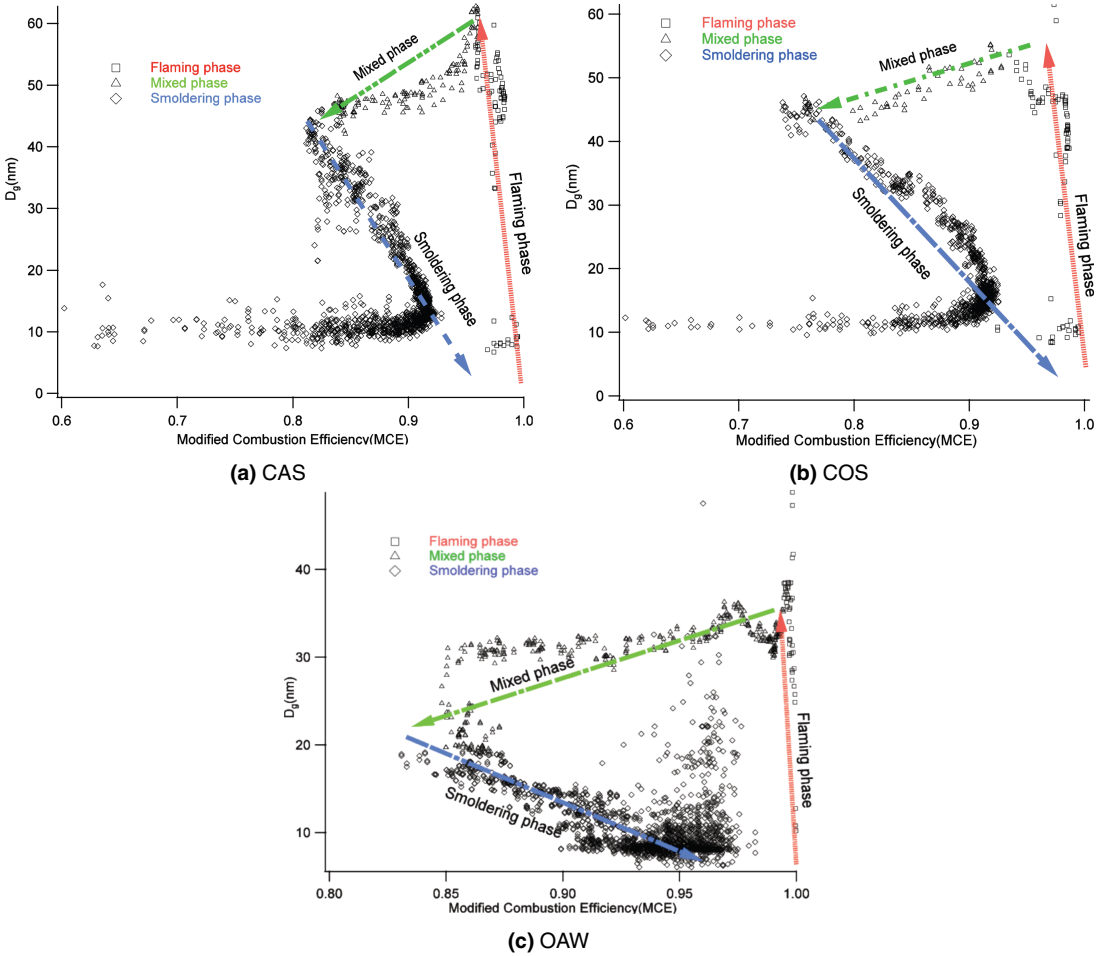

Fig. 9. MCE vs. geometric mean diameter for three typical burns.

ACPD
10, 8595–8621, 2010